Global Scientific JOURNALS

GSJ: Volume 9, Issue 7, July 2021, Online: ISSN 2320-9186
www.globalscientificjournal.com

CORROSION INHIBITION OF HYBRID POLYVINYL ALCOHOL (PVA), PROPYLENE GLYCOL (PG) AND METHYL CELLULOSE (MC) MIXED WITH ZINC AND GRAPHITE NANO PARTICLES FOR AA6061 IN SALT SOLUTION

[1]Obasi, Ibe. B. [2]Asiegbu, Daniel. A. [3]Nnanna, Lebe

[1]Department of Physics/Electronics, Federal Polytechnic, Nekede, Owerri, Nigeria
[2,3]Department of Physics Michael Okpala University of Agriculture Umudike, Nigeria

KeyWords
PVA, aluminum alloy 6061, hybrid, corrosion inhibitor, salt solution.

ABSTRACT

The corrosion inhibition effects of polyvinyl alcohol (PVA), Zn nano particles, and their mixture on AA6061 substrate in 5% KCl/NaOH mixed solution were investigated using weight-loss method, electrochemical impedance spectroscopy (EIS), polarization curve and scanning electron microscopy (SEM) for its surface morphology analysis. When PVA and Zn metal powder were mixed at varying weight ratios, the optimum inhibition efficiency was significantly increased to about 86% at a ratio of 3:1. PVA interact with the aluminum atoms at the surface to form a complex. Zn binds at this site which prevents KCl/NaOH mixture from reacting with Al alloy. Hence, an organic-inorganic inhibitor combination based on PVA and Zn nano powder can enhance the corrosion resistance of aluminum alloys as a green corrosion inhibitor.

1. INTRODUCTION

Corrosion of engineering materials particularly metals has posed a serious concern to engineers, scientists and researchers in general who are dedicated to the study of corrosion and control [1, 2, 3]. The effort on the inhibition of metals like aluminum [4, 5] that find use in many applications against corrosion is rising because of enormous losses of natural resources and finances accompanying corrosion process [6, 7, 8]. Aside the economic standpoint, corrosion control is essential likewise from environmental and aesthetics views [9, 10, 11]. Engineered aluminum are exposed to the environment which is susceptible to action of acids and bases solutions in different ways. Aluminum alloys is important for construction and operation of most household equipment services and automotive industries [12]. According to ASTM, Aluminum 6061 (AA6061) is probably the most commonly available, heat treatable aluminum alloy. AA6061 is commonly used in the manufacture of heavy-duty structures requiring good corrosion resistance, truck and marine components, railroad cars, furniture, tank fittings, general structural and high pressure applications, wire products, and in pipelines [13, 14, 15].

Corrosion inhibition techniques of metals including aluminum are anodic and cathodic inhibition [16, 17], coating [18], electroplating [19] and painting [20]. Polymers [21, 22] and nanoparticles [12, 23] have been applied in the inhibition of AA6061 against corrosion. Inhibitors are definite in action when added or present in any given corrosive environment. Several studies have established that polymers and nanoparticle are capable corrosion inhibitors because they are efficient, absence of heavy metals, less toxic, and inexpensive. Consequently, several research studies on the use of polymers mixed with nanoparticles and its corrosion inhibition properties have been conducted [23, 24, 25, 26, 27, 28].

In this study, PVA doped with Zn nanoparticles, was investigated in mixed salt environment (KCl/NaOH) at ambient temperature using weight-loss method, electrochemical impedance spectroscopy (EIS), polarization curve and scanning electron microscopy (SEM), to determine the inhibition efficiency of Zn nanoparticle in PVA matrix (PVA/Zn) on the corrosion of aluminum alloy (AA6061), and to demonstrate that AA6061 is not always corrosion resistant in all environments but can corrode when subjected to severe environments.

2. EXPERIMENTAL

2.1 Materials and Preparation

Materials used for the study were PVA with a weight-average molecular weight of 124,000 g/mol, and Zn nanopowders obtained from EastChem Industries, and AA6061 sheet of composition Si-0.92, Fe 0.395, Cu-0.263, Mn 0.0098, Mg 1.01, Cr 0.218, Ti 0.015 (ASTM) was obtained from Aliexpress online store. It was gotten in sheet of thickness, 5mm and cut into coupons of dimension, 50mm x 15mm, a hole of 3.5mm was drilled on each coupon through which a thread was passed to assistance suspension and total immersion in the media. Each coupon was prepared for the corrosion study in accordance with the ASTM-G 31 standard practice. A single environment was used for the investigation, which was a 5% standard solutions of KCl/NaOH solution obtained from the Department of Chemistry Federal Polytechnic Nekede, Owerri.

2.2 Inhibitor Preparation

100 grams of polyvinyl alcohol (PVA) was dissolved in 1 liter of water by sprinkling into the water heated to 80°C while stirring continuously using a magnetic stirrer equipped with hot plate for 20 minutes, was stirred until the solution was clear, to get the primary mixture 10% PVA solution (H0). Secondly, varying weight proportions 45g, 30g, and 15 of zinc powders were mixed into the primary solution. Four samples of the nanoparticle were prepared with different mixing ratios of zinc with this primary PVA solution. The zinc powders were dispersed in 100ml ethanol in ethanol and finally 10ml of each dispersed powders were mixed with 40ml of the polymeric solution to produce three new solutions PVA/Zn of varying Zn weight proportion denoted as H1-H3 {H1 = PVA/Zn(45g); H2 = PVA/Zn(30g) and H3 = PVA/Zn(15g)} in addition to the H0 primary solution totaling four polymeric systems. These mixtures were allowed to settle for few minutes and applied on a metal substrate by the dip-coating method that serves as sample holder and lastly, dried in a drying at oven temperature of 80°C.

2.3 Mixed Salt Immersion Test

The initial weights of the coupons were taken to the nearest 0.001g on a digital electronic weighing machine. Three different experiments were setup using the varying weight proprtion of the Zn nanoparticles in the PVA matrix plus a control (without Zn nanoparticles). The sample coupons were totally immersed in a plastic bowls containing the prepared corrosive medium. The weight loss of each coupon was determined after the period of fifty-six days. Nnanna, 2016 stated that the corrosion rate (CR), surface coverage and corrosion inhibition efficiency (I_E%) can be calculated using (Eqs. (1), (2) and (3) respectively.

$$CR(mm/y) = \frac{K\Delta W}{\rho AT} \quad (1)$$

where K is corrosion rate correction (87.6), ΔW is weight loss, ρ is density of material, A is area of the sample and t is immersion time. Surface coverage is computed from Eq. (2) as follows:

$$\theta = \frac{W_0 - W}{W_0} \quad (2)$$

here θ = surface coverage W_0 = weight without inhibitor, and W = weight with inhibitor.

$$I_E(\%) = \frac{CR_0 - CR}{CR_0} \times 100 \quad (3)$$

CR_o and CR represent the corrosion rates without and with the inhibitor, respectively.

2.4 Potential Polarization Measurements

The potential current-density curves were recorded by changing the electrode potential, E_{corr} automatically at a scan rate of 0.33 mV/s from a potential range of -800 to -300 mV. The working electrode was immersed in the test solution for 30 minutes until a steady state was achieved prior to each run. The numerical values of the variation of the corrosion current density (i_{corr}), the corrosion potential (E_{corr}), the anodic Tafel slope (β_a) and the cathodic Tafel slope (β_c) for samples H0 – H3 at ambient temperature were obtained from polarization profiles. These values were calculated from the intersection of the anodic and cathodic Tafel lines of the polarization curve at E_{corr}. The inhibition efficiency (I_E) was calculated using the following equation:

$$I_E(\%) = \frac{i_{corr} - i_{corr\,(inh)}}{i_{corr}} \times 100 \quad (4)$$

where i_{corr} and $i_{corr(inh)}$ are the corrosion current densities in the absence and presence of the inhibitor, respectively.

2.5 Electrochemical Impedance Spectroscopy (EIS) Measurements

Spectroscopy Impedance measurements were carried out in the frequency range from 10^{-1} to 10^3 Hz using an amplitude of 20 mV and 10 mV peak to peak with an AC signal at the open-circuit potential. The impedance diagrams were plotted in the Nyquist representation. Charge transfer resistance (R_{ct}) values were obtained by subtracting the high-frequency impedance. The percentage inhibition efficiency was calculated from the equation

$$I_E(\%) = \frac{\left(R_{ct} - R_{ct(inh)}\right)}{R_{ct}} \times 100 \quad (5)$$

where R_{ct} and $R_{ct(inh)}$ are the corrosion current of AA6061 without and with inhibitor respectively.

2.6 Scanning electron microscopy studies

A scanning electron microscope (SEM), model Phenom XL G2 Desktop SEM was used to analyze the morphology of the samples surface without and with inhibitor added. The sample was mounted on a metal stub and sputtered with gold in order to make the sample conductive, and the images were taken at an accelerating voltage of 10 kV using different magnifications.

3. RESULTS AND DISCUSSION

The values of inhibition efficiency (I_E%) and the corrosion rate (CR) obtained from weight loss method at different Zn nanoparticles weight proportion in PVA (PVA/Zn) are summarized in Table 1. It follows from the data that the Zn nanoparticle weight increased and corrosion inhibition increased with increase in Zn nanoparticles weight proportion. It is evident from the table that PVA/Zn composite inhibits the corrosion of AA6061 in KCl/NaOH salt solution at all the Zn nanoparticles weight proportion used in the study. Maximum inhibition efficiency was obtained for sample H2. The increased inhibition efficiency and decreased corrosion rate might be due to the Zn nanoparticle acting with the PVA as mortar and bricks around AA6061 substrate. Beyond a particular weight proportion of Zn nanoparticle (sample H3), it seemed to create holes in the coats that allow corrosion to set in, this is indicated by H3 had a lower inhibitor rate than H2.

Table 1. Weight loss measurements values of Surface coverage Corrosion rate, and Inhibition Efficiency, for the corrosion of AA6061 coated with PVA/Zn (H0-H3), in 5% KCl/NaOH salt.

Sample ID	Weight Loss (mg)	Surface Coverage θ = W0 –W /W0	Corrosion Rate (mgy)	Inhibition Efficiency (I_E %)
Blank	47.15	-	0.01518	-
H0	15.33	0.6749	0.00494	64.57
H1	12.12	0.7429	0.00390	72.86
H2	8 .63	0.8170	0.00278	81.43
H3	10.04	0.7870	0.00323	79.71

Fig. 1 represents the polarization curves for the samples in 5% KCl/NaOH salt solution. The values of corrosion potential (E_{corr}), current densities (I_{corr}), anodic Tafel slopes (β_a), cathodic Tafel slopes (β_c), and inhibition efficiency values were determined from the curves. Percentage inhibition efficiency values were 0, 61.45, 70.06, 79.21 and 75.87 respectively for the blank, H0, H1, H2 and H3 samples in that order. It is evident from the figure that the anodic Tafel slopes (β_a) remained almost constant and the cathodic Tafel slopes (β_c) varied with increasing Zn nanoparticles weight proportion in the inhibitor. This indicates that hydrogen evolution is not

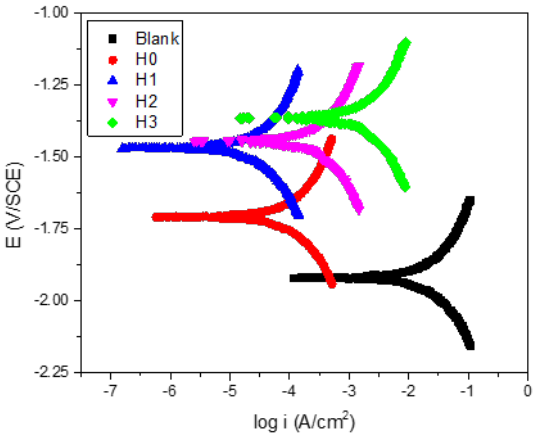

activation controlled and the addition of inhibitor changed the mechanism of cathodic hydrogen evolution reaction. In our study the maximum displacement with respect to E is less than 85mV, by literature the inhibitor can be seen as mixed type inhibitor, while maximum displacement > 85mV is anodic or cathodic type inhibitor [29]. The maximum inhibition efficiency of 79.21% is achieved at the H2 sample.

Fig. 1. Potential polarization curves for samples blank, H0 – H3 in 5% KCl/NaOH

Corrosion inhibition of AA6061 in 5% KCl/NaOH solution with and without inhibitor was investigated by electrochemical impedance spectroscopy measurements. The Nyquist representations of impedance behavior of AA6061 in the mixed salt solution with and without addition of different weight proportions of Zn nanoparticles are shown in the Fig. 2. It is observed from the figure that sam-

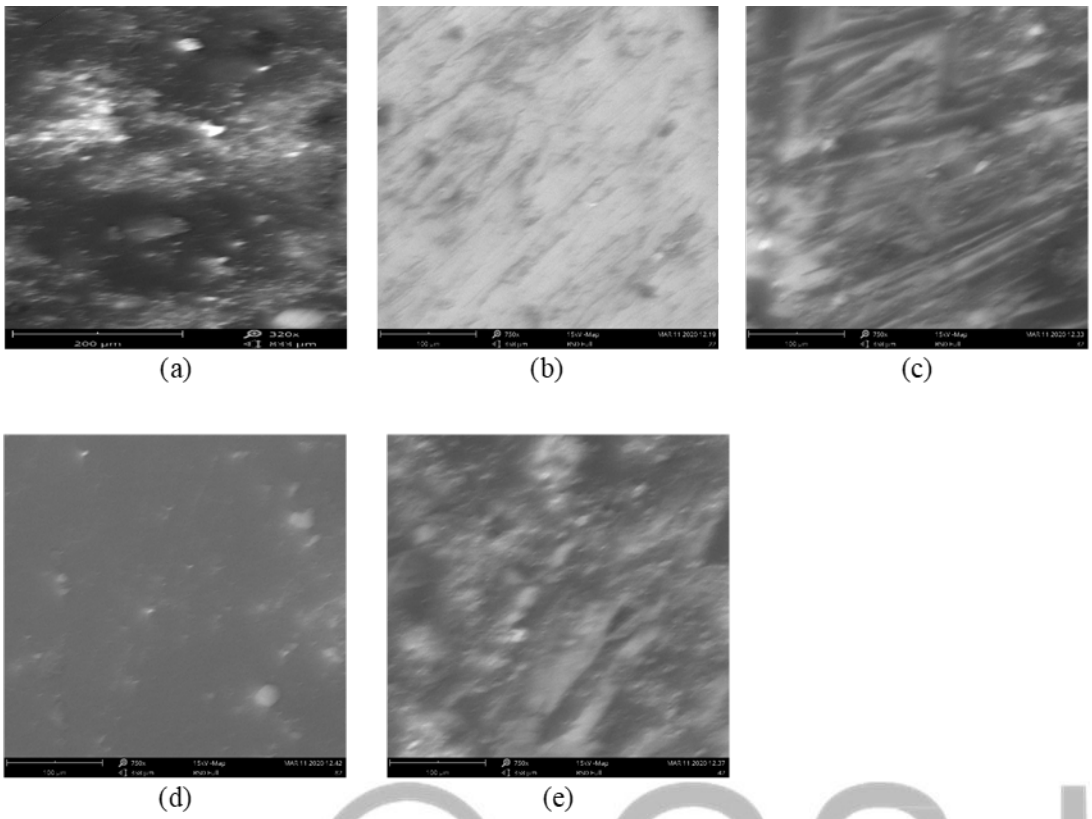

ples exhibited both large capacitive loop at higher frequency range and small inductive loop at lower frequency range. The diameter of the circle increased with increase in Zn nanoparticle content in PVA. According to [30], the higher frequency capacitive loop is due to the adsorption of inhibitor molecule.

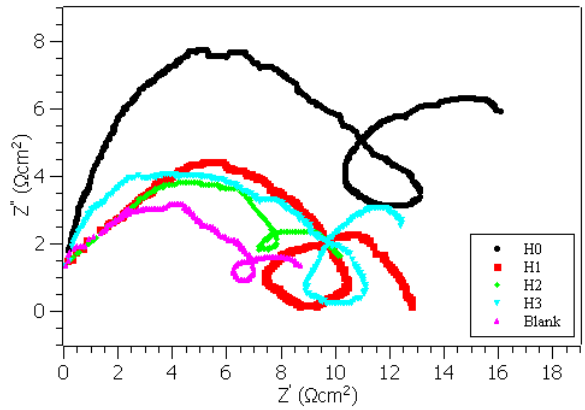

Fig. 2 Nyquist plot of AA6061 in 5% KCl/NaOH with different weight proportions of Zn nanoparticles.

SEM images shown in Fig.3, revealed that Zn nanoparticles treatment reduced the formation of pinholes and pores and decreased barrier properties. In agreement with EIS testing, SEM images showed crack-free thin films for the surfaces treated with Zn nanoparticle better than those without Zn nanoparticle treatment, which also had the better corrosion performance with H2 displaying the best performance. Zn nanoparticle doped in 10% PVA solution coating is a promising coating. It requires one layer dipping of the aluminum alloy, and then dried at oven temperature. Despite the good corrosion and adhesion properties it showed, this coating also had short self-healing properties.

Fig. 3. SEM images of the different PVA/Zn nanocomposite coated AA6061: (a) uncoated AA6061 (b) H0 coated AA6061 (c) H1 coated AA6061 (d) H2 coated AA6061 and (e) H3 coated AA6061.

4. CONCLUSION

PVA blended with varying weight proportions of Zn nanoparticles acts as a good inhibitor for the corrosion of aluminum AA6061 in 5% KCl/NaOH mixed salt solution. The results obtained from the weight loss experiment and polarization studies are in good agreement with each other. The Potential polarization curves reveal that PVA/Zn is a mixed type of inhibitor. SEM studies reveal that PVA/Zn had good corrosion resistance and adhered well with AA6061. PVA/Zn composite coating is a promising coating.

REFERENCES

[1] Kuruvila, R., Kumaran, S. T., Khan, M. A., & Uthayakumar, M. (2018). A brief review on the erosion-corrosion behavior of engineering materials. *Corrosion Reviews*, 36(5), 435-447.
[2] Pedeferri, P. (2018). Corrosion science and engineering (p. 720). Italy: Springer;
[3] Obot, I. B., Solomon, M. M., Umoren, S. A., Suleiman, R., Elanany, M., Alanazi, N. M., & Sorour, A. A. (2019). Progress in the development of sour corrosion inhibitors: Past, present, and future perspectives. *Journal of Industrial and Engineering Chemistry*, 79, 1-18.
[4] Prakashaiah, B. G., Kumara, D. V., Pandith, A. A., Shetty, A. N., & Rani, B. A. (2018). Corrosion inhibition of 2024-T3 aluminum alloy in 3.5% NaCl by thiosemicarbazone derivatives. *Corrosion Science*, 136, 326-338.
[5] Abdallah, C. S., Taryba, M., Pinto, E. R., Montemor, M. F., & Benedetti, A. V. (2019). Tannin: A natural corrosion inhibitor for aluminum alloys. *Progress in Organic Coatings*, 135, 368-381.;
[6] Abdallah, M., Gad, E. A. M., Sobhi, M., Al-Fahemi, J. H., & Alfakeer, M. M. (2019). Performance of tramadol drug as a safe inhibitor for aluminum corrosion in 1.0 M HCl solution and understanding mechanism of inhibition using DFT. *Egyptian Journal of Pet*roleum, 28(2), 173-181.; Nardeli, J. V.,
[7] Shekari, E., Khan, F., & Ahmed, S. (2017). Economic risk analysis of pitting corrosion in process facilities. International Journal of Pressure Vessels and Piping, 157, 51-62.;
[8] Yang, Y., Khan, F., Thodi, P., & Abbassi, R. (2017). Corrosion induced failure analysis of subsea pipelines. Reliability Engineering & System Safety, 159, 214-222.;
[9] Zhang, Y., Li, Q., Zhang, F., & Xie, G. (2017). Estimates of economic loss of materials caused by acid deposition in China. Sustainability, 9(4), 488.
[10] Schweitzer, P. (1983). *Corrosion and Corrosion Protection Handbook*. (Book). Marcel Dekker, Inc., 521, 1983.
[11] ASM International, ASM International. Alloy Phase Diagram Committee, & ASM International. Handbook Committee. (2005). *ASM handbook* (Vol. 13). ASM International.
[12] Fatimah, S., Kamil, M. P., Kwon, J. H., Kaseem, M., & Ko, Y. G. (2017). Dual incorporation of SiO_2 and ZrO_2 nanoparticles into the oxide layer on 6061 Al alloy via plasma electrolytic oxidation: Coating structure and corrosion properties. *Journal of Alloys and Compounds*, 707, 358-364.
[13] Fridlyander, I. N., Sister, V. G., Grushko, O. E., Berstenev, V. V., Sheveleva, L. M., & Ivanova, L. A. (2002). Aluminum alloys: promising materials in the automotive industry. *Metal science and heat treatment*, 44(9-10), 365-370.
[14] Belov, N. A., Eskin, D. G., & Aksenov, A. A. (2005). *Multicomponent phase diagrams: applications for commercial aluminum alloys*. Elsevier.
[15] Santos, M. C., Machado, A. R., Sales, W. F., Barrozo, M. A., & Ezugwu, E. O. (2016). Machining of aluminum alloys: a review. *The International Journal of Advanced Manufacturing Technology*, 86(9-12), 3067-3080.
[16] Snihirova, D., Taryba, M., Lamaka, S. V., & Montemor, M. F. (2016). Corrosion inhibition synergies on a model Al-Cu-Mg sample studied by localized scanning electrochemical techniques. *Corrosion Science*, 112, 408-417.
[17] Zeino, A., Abdulazeez, I., Khaled, M., Jawich, M. W., & Obot, I. B. (2018). Mechanistic study of polyaspartic acid (PASP) as eco-friendly corrosion inhibitor on mild steel in 3% NaCl aerated solution. *Journal of Molecular Liquids*, 250, 50-62.
[18] John, S., Salam, A., Baby, A. M., & Joseph, A. (2019). Corrosion inhibition of mild steel using chitosan/TiO_2 nanocomposite coatings. *Progress in Organic Coatings*, 129, 254-259.
[19] Reda, Y., El-Shamy, A. M., Zohdy, K. M., & Eessaa, A. K. (2019). Instrument of chloride ions on the pitting corrosion of electroplated steel alloy 4130. *Ain Shams Engineering Journal*.
[20] Luo, X., Ci, C., Li, J., Lin, K., Du, S., Zhang, H., & Liu, Y. (2019). 4-aminoazobenzene modified natural glucomannan as a green eco-friendly inhibitor for the mild steel in 0.5 M HCl solution. *Corrosion Science*, 151, 132-142.
[21] Charitha, B. P., & Rao, P. (2017). Carbohydrate biopolymer for corrosion control of 6061 Al-alloy and 6061Aluminum-15% (v) SiC (P) composite—Green approach. *Carbohydrate polymers*, 168, 337-345.
[22] Xhanari, K., & Finšgar, M. (2019). Organic corrosion inhibitors for aluminum and its alloys in chloride and alkaline solutions: a review. *Arabian Journal of Chemistry*, 12(8), 4646-4663
[23] Fatimah, S., Kamil, M. P., Kwon, J. H., Kaseem, M., & Ko, Y. G. (2017). Dual incorporation of SiO2 and ZrO2 nanoparticles into the oxide layer on 6061 Al alloy via plasma electrolytic oxidation: Coating structure and corrosion properties. Journal of Alloys and Compounds, 707, 358-364.
[24] Robert, R. J., Hikku, G. S., Jeyasubramanian, K., Jacobjose, J., & Prince, R. M. R. (2019). ZnO nanoparticles impregnated polymer composite as superhydrophobic anti-corrosive coating for Aluminium-6061 alloy. *Materials Research Express*, 6(7), 075705.
[25] Ates, M., & Dolapdere, A. (2014). Poly (3-octylthiophene) and poly (3-octylthiophene)/TiO2-coated on Al1050: electrosynthesis, characterization and its corrosion protection ability in NaCl solution. *Polymer-Plastics Technology and Engineering*, 53(17), 1768-1777.
[26] Umoren, S. A., & Eduok, U. M. (2016). Application of carbohydrate polymers as corrosion inhibitors for metal substrates in different media: a review. *Carbohydrate polymers*, 140, 314-341.

[27] Umoren, S. A., & Solomon, M. M. (2017). Synergistic corrosion inhibition effect of metal cations and mixtures of organic compounds: a review. *Journal of environmental chemical engineering*, 5(1), 246-273.
[28] Kausar, A. (2019). Corrosion prevention prospects of polymeric nanocomposites: A review. *Journal of Plastic Film & Sheeting*, 35(2), 181-202.
[29] Riggs Jr., O. L. (1973). Corrosion Inhibition, second ed., C.C. Nathan (ed)., NACE, Houston, Texas, USA
[30] Shukla, S. K. & Quraishi, M. A. (2010). The effects of pharmaceutically active compound doxycycline on the corrosion of mild steel in hydrochloric acid solution. *Corrosion. Science*. 52(2), 314-321. doi:10.1016/j.corros.2009.05.020.